Received: 20 January 2023 | Revised: 30 September 2023 | Accepted: 3 October 2023

DOI: 10.1002/pro.4803

REVIEW ARTICLE

THE PROTEIN SOCIETY WILEY

Resolution in cryogenic solid state NMR: Challenges and solutions

Ivan V. Sergeyev | **Keith Fritzsching** | **Rivkah Rogawski** | **Ann McDermott**

Columbia University, Department of Chemistry, New York, New York, USA

Correspondence
Ann McDermott, Columbia University, Department of Chemistry, 3000 Broadway, New York, New York, USA.
Email: aem5@columbia.edu

Funding information
National Institute of General Medical Sciences, Grant/Award Number: 1RM1GM145397-01; National Science Foundation, Grant/Award Number: MCB 1913885

Review Editor: Nir Ben-Tal

Abstract

NMR at cryogenic temperatures has the potential to provide rich site-specific details regarding biopolymer structure, function, and mechanistic intermediates. Broad spectral lines compared with room temperature NMR can sometimes present practical challenges. A number of hypotheses regarding the origins of line broadening are explored. One frequently considered explanation is the presence of inhomogeneous conformational distributions. Possibly these arise when the facile characteristic motions that occur near room temperature become dramatically slower or "frozen out" at temperatures below the solvent phase change. Recent studies of low temperature spectra harness the distributions in properties in these low temperature spectra to uncover information regarding the conformational ensembles that drive biological function.

KEYWORDS

cryogenic NMR, dynamic nuclear polarization, DNP, magnetic resonance, protein dynamics, solid state NMR

1 | INTRODUCTION: LOW TEMPERATURE SOLID STATE NMR

Low temperature solid state NMR spectroscopy is a powerful tool for probing biomolecules (Siegel and Anet, 1988; Tycko, 2013; Conradi, 1993). At cryogenic temperatures (<180 K) otherwise unstable species such as intermediates of chemical reactions can be trapped for study (Siegel and Anet, 1988). The use of low temperatures can also ward against sample damage during measurement, for NMR as for other structural methods such as EM or X-ray diffraction. The study of protein structure as a function of temperature has also been an important source of insights regarding biopolymer dynamics and thermodynamics (Ringe and Petsko, 2003). Recently, low temperature NMR has become additionally popular because it enables a powerful solution to detection sensitivity challenges that plague solid state NMR of complex biological samples. While the use of low temperature lowers the noise in the NMR data, a technique known as dynamic nuclear polarization (DNP) increases the signal strength by transferring polarization from unpaired electrons to nearby nuclei. If unpaired electrons are present in the sample, irradiation at the electron spin transition can facilitate hyperpolarization of the nuclei through the electron nuclear spin coupling. The theory of DNP and the various mechanisms by which polarization can be transferred to the nuclei have been reviewed elsewhere (Smith and Long, 2015; Barnes et al., 2008). The increase in nuclear polarization, and the NMR signal-to-noise ratio can improve by three orders of magnitude in principle, and signal enhancements of 250-fold have been observed for biological samples (Wenk et al., 2015). DNP enhanced NMR experiments are typically carried out at 108 K or colder. Cryogenic cooling affords a number of benefits to DNP based signal enhancement processes, including lengthening of the electronic relaxation times T_{1e} and T_{2e}, which permits effective saturation of the

electron transitions. The development of DNP methods has therefore led to a renewed interest in low temperature NMR measurements.

As is illustrated amply in the literature, low temperature NMR methods are already practically useful, particularly when combined with DNP. Applications of low temperature NMR to biopolymers, including DNP enhanced measurements, have in practice led to important insights that are not likely to have been observed at room temperature. For example, DNP-enhanced low temperature NMR studies facilitated clarification of the interface of HIV-1 V3 loop antibody (Sharpe et al., 2004), folding of the HP35 chicken villin headpiece (Hu and Tycko, 2010; Hu et al., 2009), and Alzheimer's Aβ 1–40 filbril formation (Potapov et al., 2015). Membrane proteins such as GPCRs were examined bound to native peptide ligands (Joedicke et al., 2018) and multiple bacteriorhodopsin photocycle intermediates were studied and analyzed in terms of conformation (Bajaj et al., 2007, 2010; Mak-Jurkauskas et al., 2008, 2008). DNP enhanced spectra highlight the Schiff base nitrogen of the tryptophan synthase aminoacrylate intermediate and its tautomeric exchange in the active site (Holmes et al., 2022). Large protein-nucleic acid complexes, including the Pf1 bacteriophage (Sergeyev et al., 2017) and H4 nucleosome arrays (Elathram et al., 2022) have been structurally analyzed with DNP-enhanced low temperature NMR. These and other studies illustrate the power of low temperature NMR and argue for a productive future of this subfield (Figure 1).

Despite the promise and recent impact of cryogenic NMR, one technical challenge is that the peaks for biopolymers can appear to be significantly broadened at cryogenic temperatures relative to the linewidths near room temperature. An increase in linewidth can present impediments for detailed studies. The broadening somewhat counteracts the signal-to-noise improvement from low temperature and DNP enhancement. Line broadening can defeat the ability to probe numerous sites of the protein and can undermine typical approaches to site-specific assignment of spectra. Understanding the source of the low temperature linewidth broadening and developing strategies to overcome it will enhance the potential of low temperature DNP based NMR studies. This review explores hypotheses and observations concerning the origins of the line broadening, discusses the implications for NMR analyses, and strategies for line-narrowing.

2 | LOW TEMPERATURE LINEWIDTHS AND POSSIBLE ORIGINS

2.1 | Linewidths—overview of hypotheses

Effects of temperature on linewidth have been noted for many biopolymers, typically line broadening as the temperature is dropped. The observation that low temperature lines can be broader than room temperature has been discussed in reports from relatively early biological applications of SSNMR in absence of paramagnetic radicals and signal enhancement (Jakeman et al., 1998), foreshadowing many other observations with DNP enhancement that have been reported and are discussed below. In this review we somewhat arbitrarily refer to a linewidth as "relatively narrow" if it is below 1.5 ppm for ^{13}C and below 3 ppm for ^{15}N. Linewidths frequently fall in this range but more generally can be broadened at low temperatures to over 4 ppm for ^{13}C and 3–12 ppm for ^{15}N. By contrast, linewidths at room temperature in well-resolved SSNMR studies can be as low as 0.3–0.5 ppm for ^{13}C (with contributions from J-coupling) and about 1 ppm for ^{15}N.

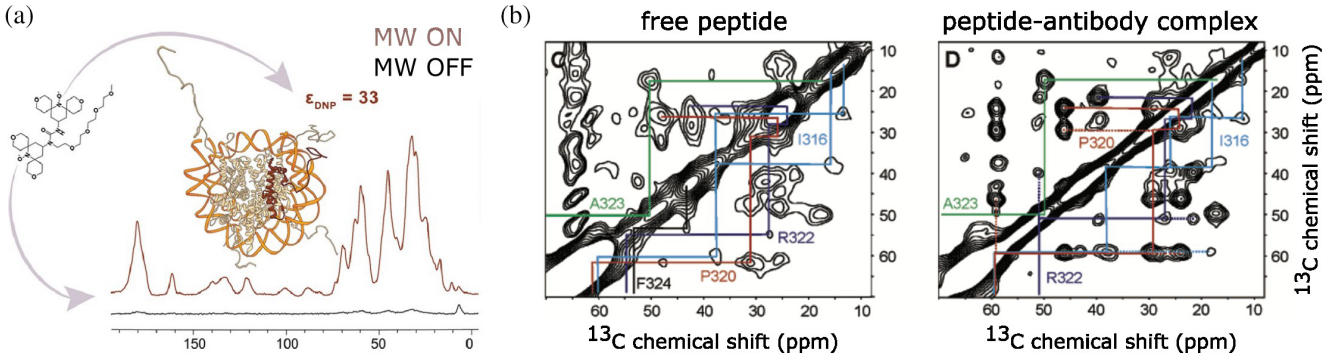

FIGURE 1 (a) DNP enhanced MAS NMR experiments of nucleosome arrays at 100 K enabled detection of long-range correlations between histone residues and DNA. (b) Low temperature NMR of an 18-residue peptide derived from the V3 loop sequence of the gp120 envelope glycoprotein of the HIV-1 (frozen glycerol/water solution) helped to define the conformation with antibody bound.

A number of hypotheses about the origin of larger linewidths at low temperature have been reported and discussed and the review is largely organized around these suggestions. Since linewidths generally contain contributions from nuclear relaxation (T_2) we begin by discussing relaxation parameters in NMR spectra of cryogenic samples (Section 2.3). We consider possible relaxation and broadening from paramagnetic centers that are added for DNP experiments (Section 2.4). Linewidths in NMR can also have contributions from conformational dynamics (Section 2.5), or from static inhomogeneous distributions of conformations (Section 2.6). Interactions with the solvent may also contribute to the linewidths (Section 2.6). Some of the linewidth contributions may be reduced with more powerful instrumentation and experimental protocols as is discussed in Section 3. In the following we explore reports from the literature that offer support for various of these hypotheses.

2.2 | Inhomogeneous and homogeneous linewidths

A key diagnostic tool in studying the origin of linebroadening is to ask whether the NMR spectra exhibit linewidths that are primarily due to differences in individual molecules, namely inhomogeneous linewidth, such as would occur in poor shimming, where various molecules are found in various magnetic fields. Alternatively, the linewidth could be a shared consistent intrinsic property of all members of the ensemble, that is, homogeneous linebroadening such as for example lifetime broadening. Though the situation is somewhat more complex when performing averaging by magic angle spinning (Mariq and Waugh, 1979) or multipulse experiments, these two limiting scenarios are conceptually useful for discerning likely mechanisms for linebroadening. Operationally, comparing the homogeneous linewidth $\Gamma = 1/(\pi T_2)$ (a function of the transverse relaxation time T_2), to the apparent full width at half maximum linewidth FWHM $= 1/(\pi T_2{}^*)$ can help to distinguish between these two limiting scenarios regarding the origin of low temperature linewidths. For homogeneous systems under ideal conditions, the apparent NMR spectral linewidth, FWHM, can be comparable to the homogeneous linewidth, Γ dictated by transverse relaxation. This relationship holds true for many cases in solution NMR. By contrast, for solid state NMR spectra, frequently the spectral lineshape FWHM linewidth differs from Γ predicted from T_2. Empirical dephasing times can be described with $T_2{}'$, the decay time measured using refocusing sequences such as by a Hahn echo or CPMG train. $T_2{}'$ can be affected by coherent line broadening mechanisms, such as heteronuclear and homonuclear dipolar or J couplings which if unresolved and undecoupled contribute additional apparent linewidth that can include homogeneous and inhomogeneous aspects. $T_2{}'$ can also be affected by molecular motion as discussed below (Section 2.5). $T_2{}^*$ or FWHM values, on the other hand, are affected by many dispersion mechanisms that can be refocused and so do not contribute to the apparent homogeneous linewidths, for example an inhomogeneous distribution of chemical shifts in the sample. These can be due to magnetic susceptibility effects including effects of poor shimming, or the effects of bulk magnetic susceptibility. Alternatively, under ideal experimental instrumental conditions the distribution of shifts may be due to inhomogeneity in conformational or local chemical environment, since different conformations typically have slightly different chemical shifts (Su and Hong, 2011; Sakellariou et al., 2003). These mechanisms typically can give rise to a distribution of chemical shifts and a lineshape that may be Gaussian or irregular, whereas the homogeneous linewidth is theoretically Lorentzian.

The question of whether homogeneous or inhomogeneous contributions to the linewidth are dominant for solid state NMR can be markedly different at room temperature versus cryogenic temperatures. Table 1 reports

TABLE 1 Transverse relaxation times for U-^{13}C,^{15}N-Pf1 samples at two temperatures, 273 K vs. 100 K, during moderate (11–12 kHz) magic angle spinning frequencies (Sergeyev et al., 2017). Values of the *effective* T_2, i.e., $T_2{}^*$, are based on the experimental half-height linewidths $T_2{}^* = \frac{1}{\pi LW}$ (the scaled inverse FWHM linewidth).

	^{13}C $T_2{}^*$ (ms)	^{15}N $T_2{}^*$ (ms)	^{13}C $T_2{}'$ (ms)	^{15}N $T_2{}'$ (ms)
273 K	4.5	2.6	5.1	5.5
100 K	1.7	1.0	10.5	41.7

Note: Values for the *refocused* homogeneous decay time T_2 (i.e., $T_2{}'$) are measured based on the decay constant in Hahn echo experiments as a function of the interpulse delays. $T_2{}'$ values lengthen considerably at low temperatures, improving the performance of many polarization transfer pulse sequence elements relative to room temperature. $T_2{}^*$ on the other hand became much shorter at low temperature, degrading the spectral resolution.

transverse relaxation rates for the coat protein from Pf1 bacteriophage prepared with AMUPOL and sensitized with DNP at 600 MHz, an example for which values are available at both room temperature and cryogenic temperatures, and both refocused relaxation values and linewidths (Sergeyev et al., 2017). When studied with DNP at 100 K, effective transverse relaxation times (T_2*) based on experimental linewidth (FWHM $\approx 1/\pi T_2$*) were considerably shorter at 100 K than room temperature (i.e., the linewidths were considerably broader at cryogenic temperatures). T_2' values on the other hand were considerably longer at 100 K than at room temperature (i.e., homogeneous linewidths are narrower at cryogenic temperatures). At low temperatures, T_2' values were up to an order of magnitude longer than T_2* (Sergeyev et al., 2017).

Analogously, ^{15}N and ^{13}C T_2' for hydrated nanocrystalline GB1 (Lewandowski et al., 2015) measured using a spin–echo pulse sequence, indicated longer coherence times at low temperature than at high temperature. Studies of ubiquitin in frozen solution (Siemer et al., 2012) follow a similar trend in that ^{13}C T_2', as measured by the Hahn echo pulse sequence, increases with decreasing temperature, while the T_2*, as measured by the linewidth, decreases with decreasing temperature. Microcrystalline samples of SH3 (Linden et al., 2011) exhibit a longitudinal relaxation time T_1 that lengthens considerably at low temperature. In another example (Su and Hong, 2011), the TAT arginine-rich cell penetrating peptide at low temperatures (238 K) demonstrated considerably broadened linewidths relative to the linewidths of crystalline solids under the same conditions. The linewidth in this case is considerably broadened, despite the fact that the refocused T_2 of both membrane peptides and crystalline sample are similar, indicating inhomogeneous disorder rather than homogeneous relaxation. Interestingly, at room temperature the linewidths of this peptide are quite narrow, indicating fast motions that lead to conformational averaging on the NMR timescale (Table 2).

Additional experimental indications support the conclusion that low temperature protein NMR linewidths are frequently primarily inhomogeneous. The ability to "burn holes" in DNP-enhanced low temperature ^{19}F NMR spectra and identify spectral components from within a broad Gaussian-like distribution (Lu et al., 2018) supports the conclusion that the low temperature linewidth is primarily inhomogeneous. Hole-burning experiments performed on low temperature NMR spectra of SH3 (Linden et al., 2011) also similarly imply that spectral broadening is inhomogenous in nature. The fact that the diagonal or autopeaks of 2D ^{13}C–^{13}C correlation spectra in many cases appear narrower than do the cross-peaks is an additional indication that inhomogenous linebroadening dominates the low temperature spectra.

It is worth noting that similar trends may be observed in low-temperature NMR of inorganic materials. For instance, significantly lengthened T_2' values were reported for MAS ^{29}Si-DNP of mesoporous silica, despite the fact that T_2* is considerably shorter at low temperature.

2.3 | Contributions from paramagnetic centers

Paramagnetic compounds cause enhanced relaxation of NMR signals associated with nearby nuclei. (Bertini et al., 2017; Clore and Iwahara, 2009) The distance dependence of this relaxation component has been

TABLE 2 Comparison of T_2' values measured for a range of samples at cryogenic conditions.

System	Relaxation rate (pulse sequence)	Nucleus type	Field (MHz)	Temp. (K)
Protofibrils, 1 mM DOTOPA-3OH-methoxy (Potapov et al., 2015)	Hahn echo T_2—14.6 ± 0.3 ms; CPMG T_2—29.3 ± 2.5 ms	^{13}C′	400	25
Protofibrils, high pH, 6.6 mM DOTOPA-3OH-Methoxy (Potapov et al., 2015)	8.8 ± 1.0 ms for Hahn echo, 15.4 for CPMG	^{13}C′	400	25
Pf1 bacteriophage with AMUPOL (Sergeyev et al., 2017)	10.5 ms (Hahn echo)	^{13}C	600	100
Pf1 bacteriophage with AMUPOL (Sergeyev et al., 2017)	41.7 ms (Hahn echo)	^{15}N	600	100
Nanocrystalline GB1 (Lewandowski et al., 2015)	>50 ms (Hahn echo)	^{13}C′	500	100
Nanocrystalline GB1 (Lewandowski et al., 2015)	>50 ms (Hahn echo)	^{15}N	500	100
Ubiquitin (Siemer et al., 2012)	~4 ms (Hahn echo)	^{13}C	750	200

Note: T_2' values are typically relatively long around 100 K, despite broad linewidths.

exploited as a source of structural information, referred to as paramagnetic relaxation enhancements (PRE). For nitroxides at room temperature and high magnetic fields, the relatively slow electron relaxation rates cause elevated nuclear R_2 relaxation rates and line broadening (Nadaud et al., 2007). It is therefore of interest to examine the contribution of paramagnetic centers to the linewidths observed in DNP spectra.

Tests for the role of PRE in low temperature NMR linewidths have been approached in a number of ways. Logically, the observation that the main source of linewidth broadening is inhomogenous (as discussed above), coupled with the expectation that paramagnetic relaxation enhancement provides *homogenous* line broadening, implies that the PRE is likely not the main source of line broadening. Conceivably, inhomogeneous behavior could nonetheless be introduced via homogeneous paramagnetic relaxation and cross-relaxation effects if other phenomena that influence the PRE such as aggregation hydration or dynamical properties vary through the sample. Studies of type 3 secretion needles showed that line broadening was not observed at room temperature with added nitroxides (Fricke et al., 2016), suggesting that PRE might also contribute marginally to low temperature linewidths. Similarly, spectra of gnnQQNY (Debelouchina et al., 2010) fibrils prepared with and without 10 mM TOTAPOL showed comparable resolution and minimal line broadening effects from the nitroxide dopant. In studies of frozen DHFR with co-localized biradical affinity tags, the nitroxides introduced signal quenching in a site-specific fashion; i.e., signals from less than 10 Å from the nitroxide have markedly reduced intensity (Rogawski and McDermott, 2017; Rogawski et al., 2017). However, for the observable sites, significant line broadening was not observed relative to samples prepared with AMUPOL. Since AMUPOL presumably had a different location than the tagged radical, the linewidths of the observable sites were not appreciably affected by radicals (as seen in Figure 2). In all of these studies, lack of dramatic broadening might be because the radicals are present at very high concentration, making electron spin exchange or diffusion an important contribution to the electron correlation timescale (McNally and Kreilick, 1981). In addition, it is worth noting that the observations mentioned above refer to the empirical linewidth, or T_2*. Since, as discussed above, $T_2^* \ll T_2'$, measurements of T_2' are expected to be more sensitive to paramagnetic dopants than linewidths. Indeed, in low temperature NMR studies of samples prepared for DNP experiments, (Corzilius et al., 2014; Linden et al., 2011). T_2' was shown to be dependent on the concentration of paramagnetic relaxant (though it was not strongly dependent on the nature of the radial). In another systematic investigation, homogeneous line widths were observed to be strongly dependent on the biradical concentration and the enhancement buildup time, and concluded that linewidths were influenced by a competition among magnetization transfer pathways (direct, indirect, and SCREAM-DNP) which in turn depend on experimental parameters such as biradical concentration or experiment repetition rate (Sergeyev et al., 2021). Measurements of ^{13}C enriched urea in samples containing 10 mM TOTAPOL showed an additional R_2 contribution due to TOTAPOL of magnitude 70 s^{-1}. Consistent with the discussions above, this effect does not parlay into a substantial contribution to the overall empirical FWHM linewidth for the typical samples probed (Potapov et al., 2015).

A novel attack on the same question involved decoupling the nearby electrons (Saliba et al., 2017). A

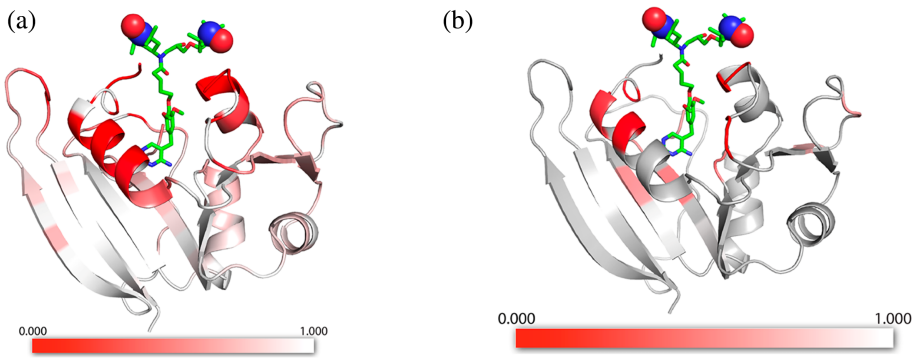

FIGURE 2 (a) Bleaching of solution state NMR (H−N HSQC) for U − ^{15}N,^{13}C-DHFR:H_2NADPH:TMP-V-T complex due to the affinity radical. A heat map is used to encode intensity ratios I_{ox}/I_{red} onto the structure, illustrating a distance dependence. (b) Low temperature SSNMR bleaching resembles the spatial patterns in solution NMR. A heat map conveys the ratio of DNP-enhanced signal intensity for specifically isotopically enriched DHFR samples with bound TMP-V-T relative to samples with exogenous AMUPol/TMP ^{13}C − ^{13}C DARR spectra (I_{TMPVT}/I_{AMUPol}).

frequency-agile gyrotron was used so that during the experiment the electron irradiation could be "hopped" from the optimal frequency for DNP (typically near the sum frequency for the nucleus and the electron) to the optimal frequency for decoupling electrons, namely on-resonance with the electron spins, a difference of ~75 MHz in frequency. In samples of trityl mixed with 40 mM uniformly ^{13}C,^{15}N enriched urea, decoupling caused line narrowing, and T_2* increases by approximately 14%. This tour de force in electron-nuclear magnetic resonance also suggests that the line broadening induced by trityl is not the main contributor of the DNP line broadening in view of the relatively modest gains in linewidth.

Another paramagnetic component in most samples is dissolved molecular oxygen, which can contribute to relaxation of NMR signals (Shikhov and Arns, 2016) particularly at low temperatures (Fyfe and Brouwer, 2004). While removing dissolved oxygen can have benefits in boosting DNP signal enhancement in samples prepared via matrix-free methods for studies of materials, nevertheless, in our hands excluding oxygen does not appreciably reduce linewidths for frozen solutions of proteins.

2.4 | Dynamic effects

Motion and dynamics have been invoked in a variety of specific ways to explain broad NMR linewidths. This hypothesis is consistent with the observed variability in linewidths from site to site within a polymer. Dynamic conformational exchange processes can contribute to larger linewidths, analogous to intermediate exchange processes in solution NMR, if molecular motion is on timescales comparable to the shift difference for the two conformers ($k_{ex} \sim \Delta\omega$). For a system in solution, $\Delta\omega$ usually refers to the change in isotropic shift for the two conformers in exchange, while for systems in solids it can refer to the anisotropic contributions to the shift, including CSA or dipolar couplings, any of which can change dramatically during conformational exchange. Changes in anisotropic couplings such as dipolar coupling during reorientation can interfere with magic angle spinning, decoupling, magnetization transfer and ultimately with signal detection over a broad range of timescales. Dynamical effects are expected to contribute to the apparent T_2' as an exchange term in transverse dephasing. Methyl groups have been shown to exhibit three-site symmetric hop motions with Arrhenius-like temperature dependence and barriers of approximately 3–4 kJ/mol depending on their local packing environment. Methyl groups would be expected to enter intermediate exchange regime for SSNMR at roughly 100 K, where $k \sim 10^4\ s^{-1} \sim \delta$ for anisotropic interactions such as the methyl CSA or the C—H couplings. The hypothesis of methyl groups being in intermediate exchange at 100 K is consonant with many experimental observations of broadened or weak lines for methyl groups. The situation for methyl CH_3 groups at 100 K with hop rates of the order of $10^4\ s^{-1}$ is analogous to that for amine NH_3 groups near or slightly below room temperatures which also have three site hop motions with rates of the order of $10^4\ s^{-1}$. The effect on interference with decoupling has been explored (Ni et al., 2017), with studies of both $^{13}CH_3$ and $^{15}NH_3$ groups in a variety of biological samples including microcrystalline peptides, the membrane protein bR, and amyloid fibrils. In this study, alanine Cβ peaks effectively disappear at approximately 112 K and reappear below 80 K, while NH_3 signals disappear at approximately 173 K. This behavior is consistent with interference of the changes in dipolar coupling due to three-fold hopping with the ^1H decoupling, when both processes are on the same timescale ($k_{ex} \sim \omega_{dip} \sim \omega_{dec}$). Notably the effect can be much attenuated with sample deuteration. In particular, for deuterated samples the Cβ-Cα crosspeak of bR was recovered. Although it is not stated in the referenced article, the disappearance of alanine Cα-Cβ crosspeaks is also clearly manifested in low temperature spectra of the Het-s amyloid fibrils (Bauer et al., 2017 Fig. 8). Similarly, for some sidechain resonances in temperature-dependent studies of Gb1 nanocrystals, intermediate exchange leads to additional broadening (Lewandowski et al., 2015). For systems that exhibit conformational exchange. benefits in sensitivity can be won from adjusting the temperature range to alter the rate constants so as to avoid interference phenomena (Li et al., 2021) (Figure 3).

2.5 | Structural inhomogeneity

Another likely explanation for broad NMR lines for many biopolymers at low temperatures is the possibility that lowering the temperature from room temperature to 100 K arrests conformational interconversions. If the various populated conformers interconvert in fast exchange near room temperature, they would collectively give rise to a single sharp line. By contrast, at 100 K they may be "frozen" meaning that they either do not interconvert or interconvert on an ultra-slow timescale and give rise to an inhomogeneous distribution of chemical shifts, with individual conformers having specific isotropic shifts. This hypothesis is consistent with the observed variability in linewidths from site to site within a polymer. In other words, linewidths are not uniform among sites in a single sample or polymer, and trends in the linewidths within a single polymer in some cases offer support for molecular-based

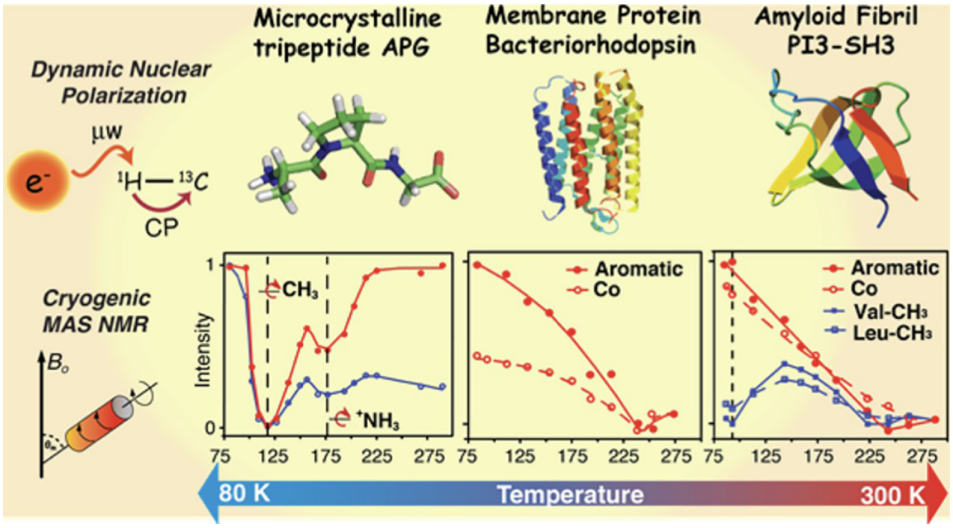

FIGURE 3 Specific loss or broadening of NMR signals at low temperature can result from exchange processes that interfere with magnetization transfer or decoupling.

mechanisms such as conformational heterogeneity or dynamics. The observation that the linewidths are primarily inhomogenous at low temperature (Section 2.2) also offers support for the hypothesis of mixtures of conformations that do not interconvert at low temperature.

The hypothesis that the broader lines at low temperature are due to static inhomogeneous mixtures of different conformations has been invoked in a number of reports to explain anomalous linewidths. In one study, the linewidth for frozen ubiquitin at low temperature (213 K) is much better fit by a Gaussian as opposed to a Lorentzian, indicating an ensemble of conformations contributing to the linewidth (Siemer et al., 2012). Frozen complexes of a HIV-1 V3 loop fragment bound to a fragment of the FV antibody (Sharpe et al., 2004) also showed patterns in linewidths suggestive of conformational order as a dominant effect (Figure 4). At 153 K most backbone carbon sites in the V3 peptide exhibited a 1.5–3 ppm reduction in linewidth upon binding, which was attributed to conformational ordering upon binding, in a model where linewidths depended on variations in the degree of side chain ordering. Another example concerns studies of protein folding: rapid cryogenic freezing was used to characterize the HP35 chicken villin headpiece, a model protein for studies of folding (Hu and Tycko, 2010; Hu et al., 2009) (Figure 4). Rapid freezing from the folded state resulted in spectra with relatively sharp lines, while rapid freezing from partly folded states with varying concentrations of guanidinium hydrochloride resulted in broad lines and the disappearance of some resonances. In another example (Potapov et al., 2015), the ^{13}C linewidths of the peptide AB 1–40 were monitored throughout its self-assembly process of fibril formation. Linewidths decreased throughout the process of assembly, from 4.4–4.7 ppm in high pH, unassembled samples, to 2.3–3.2 ppm in assembled fibrils. This progression suggests that the increasing degree of conformational order affects the linewidths in turn. In studies of the MxiH secretion needle protein by DNP enhanced NMR (Fricke et al., 2014), high resolution spectra were observed and arguments were presented that the sharp linewidths (1.1 ppm) are due to rigidity and high degree of order in the needles.

In another example, frozen solutions of DHFR exhibit a range of linewidths and offer evidence regarding the protein's response to ligand binding (Rogawski et al., 2017). Selective isotope incorporation, for example ^{13}Co-Ile/^{13}Ca-Ala enriched samples, was employed to resolve lineshapes in ^{13}C–^{13}C DARR spectra, including $^{13}C\alpha(i)$-$C'(i-1)$ correlations. In this way, the I2 C′ (resolved in the I2C′–S3Cα crosspeak) was shown to have a FWHM of 1 ppm, while two other nearby peaks have linewidths of 1.6 and 1.7 ppm, respectively. Similarly, in a sample with analogous but distinct isotopic enrichment schemes, linewidths range from 1.1 ppm for a well-resolved Cβ chemical shift, to 2.2 ppm for G67Cα. The examples described above employ strategies to resolve individual lines despite the broad low temperature linewidths such as multidimensional spectroscopy and/ or site specific sparse isotopic enrichment (Sergeyev et al., 2017).

Strong support for the importance of conformational disorder for linewidths also comes from a handful of reports of resolved splittings due to multiple conformers appearing at low temperature, which may be more easily analyzed than broadened irregular unresolved lineshapes at low temperature. Such evidence is seen in spectra of DHFR. Upon binding of the ligand trimethoprim, it is apparent that the peak corresponding to I5-Co/A6-Ca shifts and splits into two partially overlapped lines. Trimethoprim was previously shown by NMR to adopt at least two distinct orientations in the binding pocket (Polshakov et al., 1999), and the ^{15}N chemical shift of

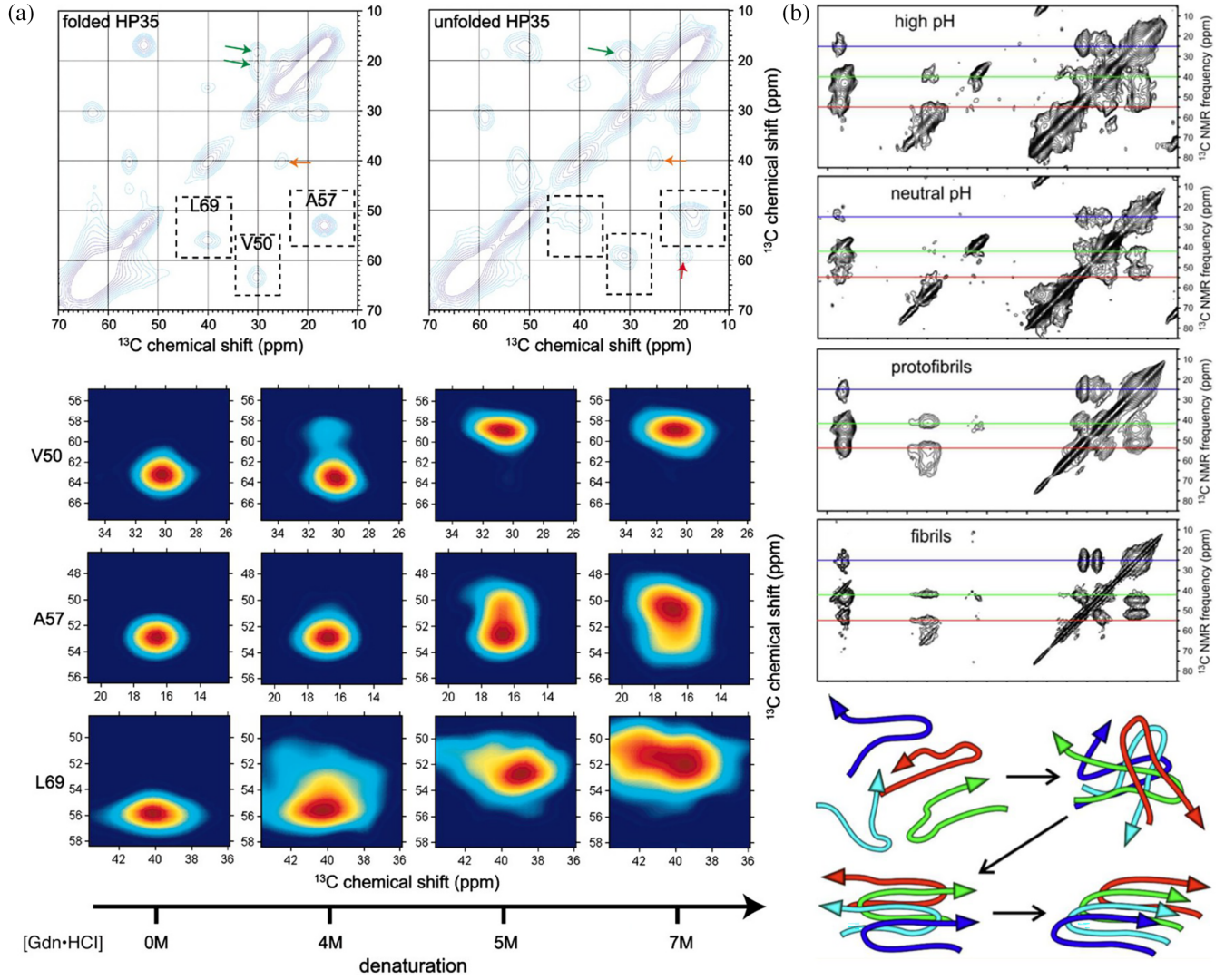

FIGURE 4 (a) Protein unfolding is associated with increased spectral linewidths. Chemical denaturation of the 35-residue villin headpiece subdomain (HP35) monitored at the site-specific level by 2D solid state NMR. (b) DNP-enhanced 2D ^{13}C SSNMR spectra of Aβ40 assemblies with selective isotopic enrichment. Note reduced disorder in Aβ40 fibrils relative to the other samples. Tertiary contacts (L34–F19) seen in several samples suggest nascent structure in the monomer.

A6-N shifts by circa 5 ppm upon TMP binding. The split chemical shifts may reflect two conformations that differ in the relation of the TMP ring and I5/A6 pair. Similarly, for microcrystalline SH3, observations of split peaks were reported and data were interpreted to be consistent with "freezing out" of multiple conformations of specific side-chains, such as A55 (Linden et al., 2011).

Conformational disorder is connected with low temperature NMR in another way: in some studies low temperatures are used to detect NMR lines that appear to be missing at RT. If peaks are missing at room temperature due to intermediate exchange conformational dynamics, then dramatically lowering the temperature could logically allow these sites to be detected. In one case an isotopic enrichment scheme was designed to detect a single site of interest in the ion channel KcsA, and while the site was undetected near room temperature, a particularly broad line was detected at 100 K, suggesting that its absence at room temperature was due to extensive exchange processes with many conformers (Howarth, 2019).

The broad linewidths are not likely to result from irreversible sample damage specific to low temperatures, such as cold denaturation. The linewidths at low temperature have been shown to be reversible, in the sense that thawing frozen DHFR samples after DNP analysis resulted in good recovery (>85%) of the protein and high quality solution NMR spectra similar to before freezing (Yi, 2023).

The hypothesis of static conformational disorder at cryogenic temperatures has also been invoked in discussion of NMR spectra of small crystalline molecules. N-f-MLF peptides exhibit no changes in linewidth for the more dynamically hindered form of the peptide (N-f-MLF-oME),

while in N-f-MLF-OH the dynamics of the system led to lineshape changes at lower temperatures. Two co-existing forms of the peptide at low temperature differ by local changes in conformation (Barnes et al., 2010), implying a relationship between conformational disorder, dynamics and distributions of chemical shifts in low temperature NMR spectra. For crystals of sodium ibuprofen (Concistrè et al., 2014), peaks associated with hydrophilic sites remained relatively sharp, while a hydrophobic region with a flexible isobutyl group displayed inhomogenous broadening at low temperature. For this sample, relatively sharp refers to linewidths of approximately 2 ppm. Studies of crystals of sodium ibuprofen (Concistrè et al., 2014) indicate dehydration over a range of temperatures. Among four resonances that displayed inhomogeneous broadening, the extent of the broadening could be correlated with the intermediate exchange dynamics and motions known to be carried out by each functional group. DFT chemical shift calculations also indicated a correlation between the isotropic chemical shift distributions populated above the freezing temperature and linewidths observed at cryogenic temperatures. Possibly, in this case a complex interplay between conformation distributions, solvent interactions, and dynamics affects the linewidths.

The data offer hints regarding the timescale of conformational interconversion for typical examples. Hypothetically, for most cases discussed above the exchange process interconverting the conformers is sub-ns at RT, in other words well-averaged and in the fast limit for NMR detection. By contrast, for most cases the dynamics are supra-ms at 100 K, in other words in the ultra-slow limit. This dramatic change in timescales with temperature could be possibly due to a steep activation energy. Perhaps more intuitively the steep change in rate for many samples could be due to a strong effect of the solvent phase change on interconversion dynamics, or the glass transition of the protein (Ringe and Petsko, 2003).

A direct test for the hypothesis of conformational heterogeneity underlying the broad lines at low temperature was conducted by measuring torsion angles for a single well-structured site in a globular proteins, contrasting the torsion angle for various positions within the broad lineshape (Yi, 2023) (Figure 5). The I60-I61 amide bond of DHFR is in a well-structured beta sheet. This site was studied in a frozen solution of the DHFR:trimethoprim ligand complex. ^{15}N–$^{13}C'$ correlation spectra of samples prepared with selective ^{15}N and ^{13}C isotopic enrichment in Ile only allowed this unique I–I pair to be detected in a N–C correlation spectrum without interference from other amides, revealing the lineshape clearly. Using the N($i+1$)–C(i) correlation spectrum as a "working fingerprint plane", the torsion angle Ψ_I was measured in a third pseudo-dimension, revealing a range of over 50° in Ψ values for this amide group, despite the fact that it is located in a well-structured beta sheet. The Ψ value for residue i correlates strongly with the N(i) isotropic shift, both experimentally and in QM/MM simulations. This study offers strong supportive evidence for conformational degrees of freedom leading to inhomogeneous linewidth at low temperature, though further studies on other sites are needed.

2.6 | The role of the solvent

Several studies have explored the role of aqueous solvent in cryogenic line broadening. Water in protein samples is often divided into three types: bulk water with a freezing point near 0°C, hydration water that directly surrounds the protein molecule with a depressed freezing point (−25 to −60°C), and unique protein bound, structural waters with long residence times. Studies of GB1 (Lewandowski et al., 2015) as a function of temperature indicated two turning points or discrete changes in

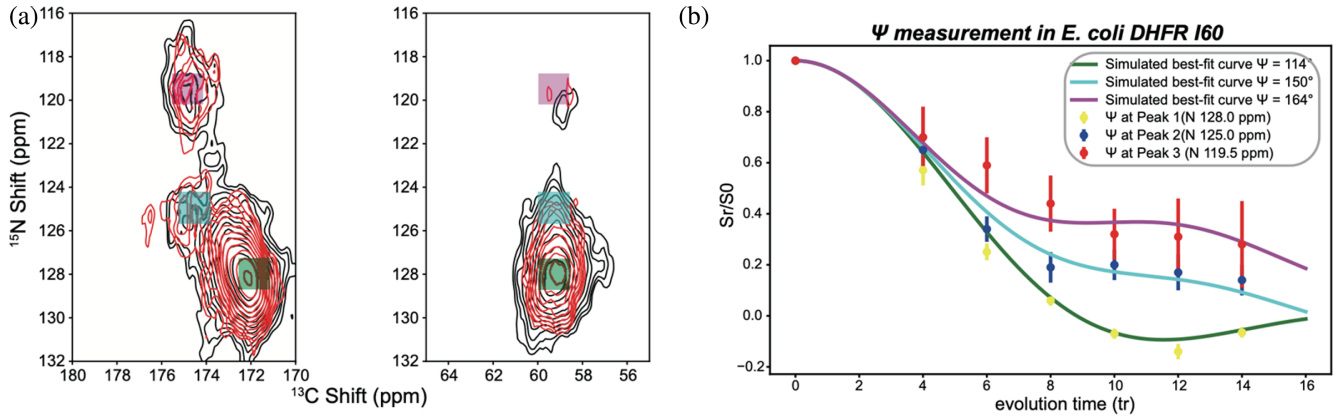

FIGURE 5 (A) Various "basins" can be identified within the broad spectral lineshape of I60 C′–I61N correlation spectra. (b) Torsion angle restraints from three "basins" within the lineshape of I60 C′–I61N correlation spectra.

dynamic behavior and linewidth. At 220 K changes were putatively associated with freezing of the hydration water, while at 160 K changes in side chain dynamics coupled to solvent were invoked. Studies of Het-S fibrils (Bauer et al., 2017) also report a pattern in solvent exposed versus hydrophobically buried residues, namely that the former broaden at around 240 K in a relatively sharp transition, near the freezing point of the hydration water, while the latter are still observable even at low temperature. In the study of DNP-enhanced low temperature SSNMR spectra of the major coat protein of the Pf1 bacteriophage, in the context of the whole phage particle, a broad range of linewidths for backbone sites was reported, all much broader than the corresponding room temperature peaks (Sergeyev et al., 2017). Chemical shift perturbations and line broadening were shown to be strongly correlated to solvent exposure. The narrower lines in the interior suggest the presence of fewer conformational states or better annealing of the sample into a single conformation during freezing. The broader lines for solvent exposed sites suggest that multiple states with comparable energetics co-exist at the freezing point. Studies of frozen complexes of a HIV-1 V3 loop fragment bound to a fragment of the FV antibody (Sharpe et al., 2004) also demonstrated that solvent exposed residues can be broadened more significantly. Studies of nanocrystals and amyloid fibrils also led to the conclusion (Debelouchina et al., 2010) that residues in contact with water experienced more significant inhomogeneous broadening than other residues. The choice of cryoprotectants and glassing agents and lipids (for membrane proteins) was also explored recently in connection with the choice of polarization agents (Tran et al., 2020).

Solvent-free systems also support this line of reasoning. Microcrystals of alanyl-prolyl-glycine (APG) (Ni et al., 2017; Barnes et al., 2010) show resolution comparable to that observed at room temperature, with linewidths of 0.28 ppm at 80 K. As a consequence, splittings due to J-couplings were resolved, which is typically not seen in solid state NMR. Other microcrystalline solids studied by DNP also exhibit narrow linewidths, including powdered glucose which has a linewidth of 0.33 ppm at 100 K, comparable to a linewidth of 0.28 at 298 K (Björgvinsdóttir et al., 2018), and crystalline L-histidine which had a linewidth of 52 Hz. These solids were wet with a biradical solution prepared in tetrachloroethane (TCE), which does not dissolve the crystals themselves. Crystals of N-MLF, which are solvent free, also show little transition in linewidths between 200 and 240 K (Bajaj et al., 2009).

Given that water as a solvent appears to play an essential role in the linewidth, the form of ice that is developed might be important. In this regard, for aqueous preparations cosolutes can be expected to be quite influential, and the freezing rate might also be important. A number of strategies for cryoprotection have been reported, and the effectiveness of cosolutes for globular proteins for preserving native structure and ensuring narrow low temperature NMR linewidths was surveyed; the study overall demonstrated benefits to low temperature NMR linewidths when cosolutes are optimized (Jakeman et al., 1998). In another study (Lee and Hong, 2014), the efficacy of various membrane cryoprotectants concluded that DMSO is effective at inducing more homogeneous preparations and appears to immobilize the polar headgroup of the lipid. Freezing rates can affect the type of ice formed, and are important for obtaining excellent specimens for other biophysical methods, so it is natural to suppose that freezing rates might affect the low temperature NMR linewidths. Hexagonal ice formation is associated with slow freezing and may cause misfolding and sample heterogeneity, while hexagonal ice formation is suppressed in rapid freezing and glassy ice instead may be formed, potentially resulting in a more homogeneous native-like conformational distribution. It is also likely that rapid versus slow freezing protocols may affect the ability of the system to anneal to preferred lowest enthalpy states. These ideas were tested using a very rapid freezing protocol involving depositing ("shooting") nanoliter solution droplets onto copper wheels that are thermally equilibrated with liquid nitrogen. In the case of frozen solutions of *E. coli* DHFR, little effect of slow versus rapid freezing on linewidth was seen, as illustrated in Figure 6. On the other hand in the same experiments, rapid freezing was shown to have useful effects on the polarization enhancement (not shown), enabling good enhancement ratios with little glycerol included.

3 | EXPERIMENTAL STRATEGIES FOR LINE NARROWING

For the DNP-NMR spectroscopist confronted with a sample with intrinsic broad lines, a variety of experimental strategies have been presented in the literature for narrowing linewidths and, as discussed below, improvements have been noted in many cases. Presumably, increases in resolution will be sample-dependent and determined by the types of linebroadening that are relevant for a particular sample.

Increasing the static magnetic field strength is a well-known strategy for narrowing NMR lines. This is beneficial because higher fields increase the spectral dispersion, while broadening mechanisms may be only weakly field dependent. For example, in going from 600 to 800 MHz, DNP linewidths of type III secretion needles decreased by about 25% (in ppm). Similarly, for a sample of uniformly

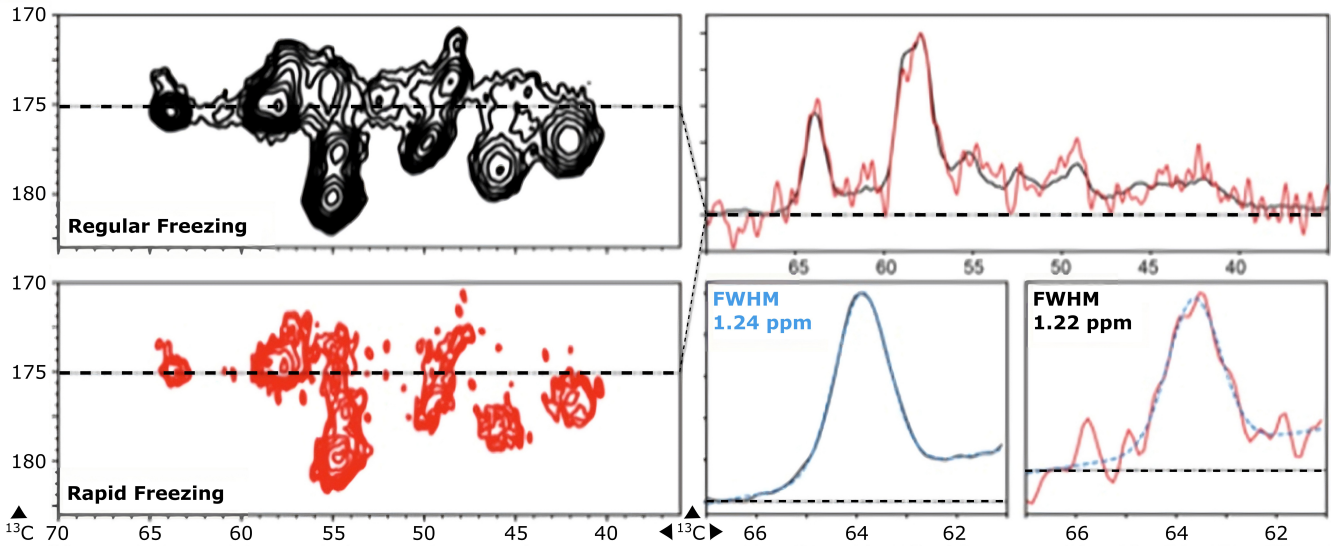

FIGURE 6 DNP NMR spectra at 105 K are compared for rapid freeze quench samples vs. with normal freezing samples. For this study, DHFR was selectively isotopically enriched with U ^{13}C in four amino acids, LAPG. FWHM linewidths are indistinguishable for all sites in this case.

isotopically enriched Aβ40 fibrils, linewidths for resolved peaks were similar at room temperature and cryogenic temperatures (ca. 100 K), and by increasing the magnetic field strength from 9.4 T to 20.2 T (400–850 MHz ^{1}H frequency), resolution improved dramatically (Lopez Del Amo et al., 2013). Other studies also suggest that an increased magnetic field strength can offset the deleterious effect of lowering temperature (Liao et al., 2016). This observation is at odds with the observation above that the linewidth is mainly inhomogeneous at low temperature, so further investigations are needed.

Sample deuteration can narrow lines if the primary cause of broadening is associated with ineffective proton decoupling (e.g., due to hardware challenges, the presence of paramagnetic centers, or motion). For example, when intermediate exchange dynamics causes line broadening through interference with proton decoupling, deuteration of the protein can recover the methyl ^{13}C–^{13}C correlations (Ni et al., 2017).

It has been shown that increasing the rotor frequency for MAS, ω_r, can improve resolution in solid state NMR experiments. Increasing ω_r enables effective averaging of homonuclear proton dipolar couplings, resulting in narrowed linewidths. In one study, the MAS frequency was increased to 40 kHz (compared to typical MAS frequencies between 8 and 13 kHz for DNP experiments) and improvement in the DNP enhancement ($\varepsilon = I_{on}/I_{off}$, where I is the signal intensity and on versus off refers to the electron microwave irradiation for DNP) resulted (Chaudhari et al., 2017). Moreover, spinning with a frequency of 40 kHz increased coherence lifetimes for ^{29}Si significantly. At $\omega_r = 40$ kHz the T_2' CPMG values were ~3× longer than those measured at 10 kHz. Similarly, increasing the MAS frequency from 11 kHz to 25 kHz, the T_2' of Pf1 lengthened by approximately 30% (Sergeyev et al., 2017). Also, for frozen DHFR in a glassy matrix of D_2O/d_8-glcyerol, with site-selective enrichment, T_2' lengthens from 10 ms to 14.4 ms, an increase of approximately 40% with a comparable increase in ω_r. This results in line narrowing by 45 ± 10 Hz in ^{13}C–^{13}C peaks in a PDSD-DARR spectra with 100 ms of DARR mixing.

Another consideration is the magnetic field homogeneity (Fritzsching et al., 2018) which can change when the sample is cooled. DEMA, a tertiary amine that remains a liquid at 130 K, can be used to shim the magnet at 130 K, which is considerably closer to the temperatures typically used for DNP experiments. Shimming under appropriate conditions decreases the contribution of magnetic field inhomogeneity to the linewidth and results in overall spectral improvement particularly for larger rotors.

In some cases, introducing more chemical shift dimensions can provide resolution between sites, thus allowing for biopolymer site specific analysis despite poor linewidths. This is particularly effective with judicious choices of digitization dimensions. Given that ^{15}N amidic backbone sites are particularly broad, their digitization may be omitted (even if transfer through the N is utilized). This approach presents an inherent challenge, namely implying multiple transfer steps. The properties of low temperature NMR spectra may lend themselves to such a strategy as follows: despite short T_2^* values, long T_2' values are typically observed at low temperature, allowing for efficient magnetization transfers in novel complex SSNMR pulse sequences. Accordingly, many groups have developed modifications of the typical assignment and tertiary contact workflow to enable

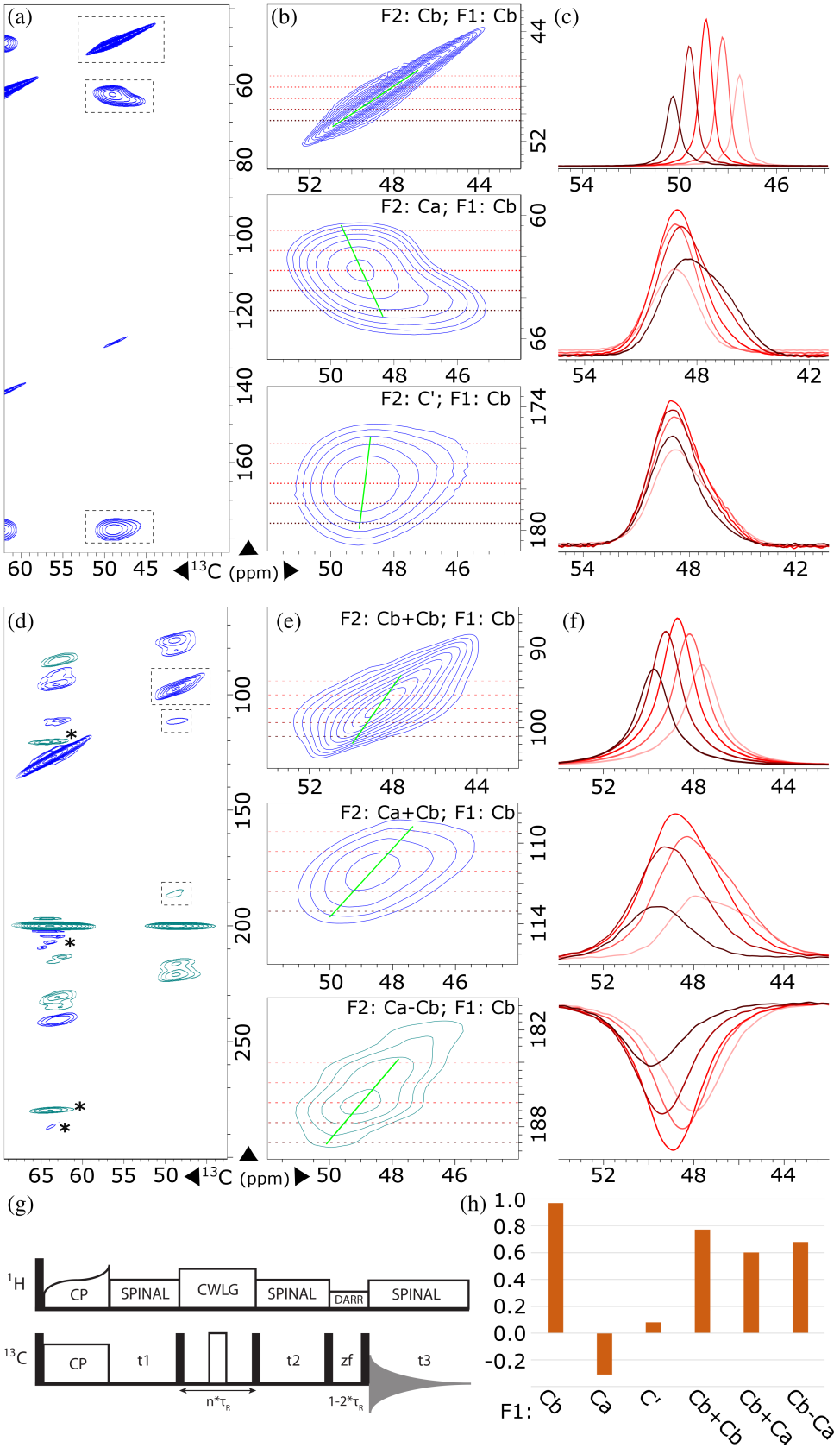

FIGURE 7 Legend on next page.

structural studies at low temperatures: the long-range 2D, lots of transfers. Capitalizing on this opportunity, the S3 pulse sequence, correlates side-chain resonances through a series of long range polarization transfers, which are only feasible due to the enhanced DNP signal strength as well as the long T_2' values (Sergeyev et al., 2017).

Going forward, other data collection and signal processing strategies may also have promise to narrow resonances. For example, if the origin of the broad line is bulk susceptibility, the shifts of neighboring sites are expected to be strongly correlated. If this is the case, zero quantum spectra are expected to have better resolution than single quantum spectra. Work from Pines, Warren and others demonstrates that, as expected, zero quantum coherences, in many cases, are not inhomogenously broadened by bulk susceptibility mechanisms (Munowitz and Pines, 1986; Hall and Norwood, 1986, 1987), and refocused ZQ spectra can show excellent resolution (Sakellariou et al., 2003). Alternatively, correlation spectra have been observed to exhibit significantly narrower peaks than 1D spectra in DNP samples of some pharmaceuticals (Hanrahan et al., 2017). Analogous approaches may have benefit for low temperature NMR, particularly if inhomogenous broadening reflects structural disorder, and the shifts are systematic with structure. In this case, the shifts of directly bonded sites are frequently anticorrelated, and MQ spectroscopy can have benefit in removing bulk susceptibility while enhancing local effects of interest. A proof of concept example is shown in Figure 7, where single quantum coherences for proline in solution are correlated to sum or difference spectra. The data were recorded using GFT (Kim and Szyperski, 2003) in DNP-enhanced spectra at 105 K. Here, sum frequency lines are narrower than expected based on the direct/SQ linewidths, consistent with anticorrelated shifts for neighboring carbons within a conformational distribution.

4 | INSIGHTS FROM LOW TEMPERATURE SHIFT DISTRIBUTIONS

As outlined in the discussions above, one of the leading hypothesis for the larger linewidths at low temperature is that the sample contains a distribution of conformations associated with different isotropic shifts. The various conformations are not in rapid exchange at 100 K (inhomogeneous distribution), and are presumed to exist in rapid exchange with each other at 300 K (homogeneous distribution). If this hypothesis is correct, the distribution of isotropic shifts at low temperature could provide insights regarding conformational ensembles of biopolymers. This suggestion accords well with prior studies on chemical shift prediction for biopolymers, where the isotropic shift predictions are in better agreement with experimental values if an average over the broad distribution of isotropic shifts expected for thermal conformational ensembles is performed (Perez-Conesa et al., 2021; Robustelli et al., 2012; Li and Brüschweiler, 2012).

With this in mind, a handful of studies have explored the connection between low temperature linewidth and conformational ensembles using computational tools, with molecular dynamics based sampling, and QM/MM calculations of NMR shifts for selected snapshots along the MD trajectory (Yi, 2023; Gupta et al., 2019). Good agreement between computed and experimentally observed lineshapes (isotropic shift distributions) offers strong support for the hypothesis that linewidths are dominated by conformational heterogeneity, and suggests

FIGURE 7 Panels (a-c) Expansions from a ^{13}C-^{13}C DARR spectra of DNP enhanced cryo MAS spectra of U-^{13}C,15N proline, showing diagonal and off-diagonal peak shapes commonly observed in NMR experiments performed at cryogenic temperatures. Horizontal slices through the peaks in (b) at the indicated frequencies are shown in (c). Peak slopes are defined as the ratio, Df2/Df1, of the change in maximum intensity position in the direct dimension with respect to the position in the indirect dimension. Slopes are indicated as light green guide-lines through each peak's maximum and are summarized in (h). The autopeak is notably narrow in slices at any position, consistent with the observation of transverse relaxation rates much longer than the inverse peak envelope width ($T_2^*<<T_2$ indicating dominant inhomogeneous linewidth mechanism). Negative peak slope for the Ca—>Cb cross-peak indicates that the chemical shift distributions of neighboring nuclei are anti-correlated. Panels (d-g) GFT-encoded h(CC)C sum and difference spectra DNP enhanced cryo MAS spectra of U-^{13}C,^{15}N proline, wherein two ^{13}C coevolution periods separated by a mixing time make up the indirect dimension, allowing magnetization to evolve at sum and difference chemical shift distributions across the lineshape. NMR pulse sequence is shown schematically in (g). Expanded crosspeaks (e) and corresponding horizontal slices at indicated frequencies (f) indicate that the Ca shift is strongly anticorrelated to the corresponding Cb shift when comparing various microstates across the distribution. Anticorrelated chemical shifts within the distributions lead to diagonal-like peak shapes for the Ca-Cb—> Cb with a somewhat larger peak width for the difference frequency indirect measurement as for the sum frequency. A likely (and testable) explanation for these observations is that proline has conformational microstates when frozen, and within these conformations directly bonded carbons such as Ca and Cb have anticorrelated isotropic chemical shifts. By contrast, if the linewidth were dominated by correlated effects such as local susceptibility of dipolar fields, the difference frequency width would be expected to be notably narrower.

that this (Li and Brüschweiler, 2012) will be a promising line of inquiry going forward.

5 | CONCLUSIONS AND PROSPECTS

Low temperature NMR has the potential to provide rich site-specific details regarding biopolymer structure and function, but broad spectral lines compared with room temperature NMR can sometimes present practical challenges. Among a number of other hypotheses regarding the origins of line broadening, one common explanation is the static inhomogeneous conformational distributions that result from reduced motions in the solvent and biopolymer at low temperatures. Going forward, studies of low temperature spectra are likely to yield insights into the conformational ensembles that underlie biological function.

AUTHOR CONTRIBUTIONS

Ivan V. Sergeyev: Conceptualization (equal); data curation (equal); formal analysis (equal); investigation (equal); writing – review and editing (equal). **Keith Fritzsching:** Conceptualization; data curation (equal); formal analysis; investigation. **Rivkah Rogawski:** Conceptualization (equal); data curation (equal); formal analysis (equal); investigation (equal); writing – original draft (equal). **Ann McDermott:** Conceptualization (equal); data curation (equal); formal analysis (equal); funding acquisition (equal); investigation (equal); methodology (equal); writing – original draft (equal); writing – review and editing (lead).

ACKNOWLEDGMENTS

This work was supported by a grant from the NSF (MCB 1913885), and a Biomedical Technology Development and Dissemination Center grant from the NIH (1RM1G M145397-01).

DATA AVAILABILITY STATEMENT

Data available on request from the authors.

ORCID

Ivan V. Sergeyev https://orcid.org/0000-0001-6008-6633
Ann McDermott https://orcid.org/0000-0002-9249-1649

REFERENCES

Bajaj VS, Mak-Jurkauskas ML, Belenky M, Herzfeld J, Griffin RG. Functional and shunt states of bacteriorhodopsin resolved by 250 GHz dynamic nuclear polarization–enhanced solid-state NMR. Proc Natl Acad Sci. 2009;106:9244–9.

Bajaj VS, Mak-jurkauskas ML, Belenky M, Herzfeld J, Griffin RG. DNP enhanced frequency-selective TEDOR experiments in bacteriorhodopsin. J Magn Reson. 2010;202:9–13.

Bajaj VS, van der Wel PCA, Griffin RG. Observation of a low-temperature, dynamically driven structural transition in a polypeptide by solid-state NMR spectroscopy observation of a low-temperature, dynamically driven structural transition in a polypeptide by solid-state NMR. 2009;125:118–28.

Barnes AB, Corzilius B, Mak-Jurkauskas ML, Andreas LB, Bajaj VS, Matsuki Y, et al. Resolution and polarization distribution in cryogenic DNP/MAS experiments. Phys Chem Chem Phys. 2010;12:5861–7.

Barnes AB, De Paëpe G, van der Wel PCA, Hu K-N, Joo C-G, Bajaj VS, et al. High-field dynamic nuclear polarization for solid and solution biological NMR. Appl Magn Reson. 2008;34:237–63.

Bauer T, Dotta C, Balacescu L, Gath J, Hunkeler A, Böckmann A, et al. Line-broadening in low-temperature solid-state NMR spectra of fibrils. J Biomol NMR. 2017;67:51–61.

Bertini I, Luchinat C, Parigi G, Ravera E. Relaxation. NMR of paramagnetic molecules, applications to metallobiomolecules and models. 2nd ed. Elsevier; 2017. p. 77–126. https://doi.org/10.1016/B978-0-444-63436-8/00004-1

Björgvinsdóttir S, Walder BJ, Pinon AC, Reddy Yarava J, Emsley L. DNP enhanced NMR with flip-back recovery. J Magn Reson. 2018;288:69–75.

Chaudhari SR, Wisser D, Pinon AC, Berruyer P, Gajan D, Tordo P, et al. Dynamic nuclear polarization efficiency increased by very fast magic angle spinning. J Am Chem Soc. 2017;139:10609–12.

Clore GM, Iwahara J. Theory, practice, and applications of paramagnetic relaxation enhancement for the characterization of transient low-population states of biological macromolecules and their complexes. Chem Rev. 2009;109:4108–39.

Concistrè M, Carignani E, Borsacchi S, Johannessen OG, Mennucci B, Yang Y, et al. Freezing of molecular motions probed by cryogenic magic angle spinning NMR. J Phys Chem Lett. 2014;5:512–6.

Conradi M. Low-temperature NMR techniques. Concepts Magn Reson A. 1993;5:243–62.

Corzilius B, Andreas LB, Smith AA, Ni QZ, Griffin RG. Paramagnet induced signal quenching in MAS-DNP experiments in frozen homogeneous solutions. J Magn Reson. 2014;240:113–23.

Debelouchina GT, Bayro MJ, van der Wel PCA, Caporini MA, Barnes AB, Rosay M, et al. Dynamic nuclear polarization-enhanced solid-state NMR spectroscopy of GNNQQNY nanocrystals and amyloid fibrils. Phys Chem Chem Phys. 2010;12:5911–9.

Elathram N, Ackermann BE, Debelouchina GT. DNP-enhanced solid-state NMR spectroscopy of chromatin polymers. J Magn Reson Open. 2022;10–11:100057.

Fricke P, Demers JP, Becker S, Lange A. Studies on the MxiH protein in T3SS needles using DNP-enhanced ssNMR spectroscopy. ChemPhysChem. 2014;15:57–60.

Fricke P, Mance D, Chevelkov V, Giller K, Becker S, Baldus M, et al. High resolution observed in 800 MHz DNP spectra of extremely rigid type III secretion needles. J Biomol NMR. 2016;65:121–6.

Fritzsching KJ, Itin B, McDermott AE. N,N-Diethylmethylamine as lineshape standard for NMR above 130 K. J Magn Reson. 2018;287:110–2.

Fyfe CA, Brouwer DH. Effect of molecular oxygen on the variable-temperature 29Si MAS NMR spectra of zeolite-sorbate complexes. J Am Chem Soc. 2004;126:1306–7.

Gupta R, Zhang H, Lu M, Hou G, Caporini M, Rosay M, et al. Dynamic nuclear polarization magic-angle spinning nuclear magnetic resonance combined with molecular dynamics simulations permits detection of order and disorder in viral assemblies. J Phys Chem B. 2019;123:5048–58.

Hall LD, Norwood TJ. High resolution NMR measurements in inhomogenous magnetic fields: use of the SECSY pulse sequence. J Chem Soc Chem Commun. 1986;20:1508–10.

Hall LD, Norwood TJ. Measurement of high-resolution NMR spectra in an inhomogeneous magnetic field. J Am Chem Soc. 1987;109:7579–81.

Hanrahan MP, Venkatesh A, Carnahan SL, Calahan JL, Lubach JW, Munson EJ, et al. Enhancing the resolution of ^{1}H and ^{13}C solid-state NMR spectra by reduction of anisotropic bulk magnetic susceptibility broadening. Phys Chem Chem Phys. 2017;19:28153–62.

Holmes JB, Liu V, Caulkins BG, Hilario E, Ghosh RK, Drago VN, et al. Imaging active site chemistry and protonation states: NMR crystallography of the tryptophan synthase α-aminoacrylate intermediate. Proc Natl Acad Sci U S A. 2022;119:e2109235119.

Howarth GS. Potassium channel KcsA and its lipid environment. Columbia University; 2019.

Hu KN, Havlin RH, Yau WM, Tycko R. Quantitative determination of site-specific conformational distributions in an unfolded protein by solid-state nuclear magnetic resonance. J Mol Biol. 2009;392:1055–73.

Hu KN, Tycko R. What can solid state NMR contribute to our understanding of protein folding? Biophys Chem. 2010;151:10–21.

Jakeman DL, Mitchell DJ, Shuttleworth WA, Evans JNS. Effects of sample preparation conditions on biomolecular solid-state NMR lineshapes. J Biomol NMR. 1998;12:417–21.

Joedicke L, Mao J, Kuenze G, Reinhart C, Kalavacherla T, Jonker HRA, et al. The molecular basis of subtype selectivity of human kinin G-protein-coupled receptors. Nat Chem Biol. 2018;14:284–90. https://doi.org/10.1038/nchembio.2551

Kim S, Szyperski T. GFT NMR, a new approach to rapidly obtain precise high-dimensional NMR spectral information. J Am Chem Soc. 2003;125:1385–93.

Lee M, Hong M. Cryoprotection of lipid membranes for high-resolution solid-state NMR studies of membrane peptides and proteins at low temperature. J Biomol NMR. 2014;59:263–77.

Lewandowski JR, Halse ME, Blackledge M, Emsley L. Direct observation of hierarchical protein dynamics. Science. 2015;1979(348):578–81.

Li DW, Brüschweiler R. PPM: a side-chain and backbone chemical shift predictor for the assessment of protein conformational ensembles. J Biomol NMR. 2012;54:257–65.

Li Y, Chaklashiya R, Takahashi H, Kawahara Y, Tagami K, Tobar C, et al. Solid-state MAS NMR at ultra low temperature of hydrated alanine doped with DNP radicals. J Magn Reson. 2021;333:107090.

Liao SY, Lee M, Wang T, Sergeyev IV, Hong M. Efficient DNP NMR of membrane proteins: sample preparation protocols, sensitivity, and radical location. J Biomol NMR. 2016;64:223–37.

Linden AH, Franks WT, Akbey Ü, Lange S, van Rossum BJ, Oschkinat H. Cryogenic temperature effects and resolution upon slow cooling of protein preparations in solid state NMR. J Biomol NMR. 2011;51:283–92. https://doi.org/10.1007/s10858-011-9535-z

Lopez Del Amo JM, Schneider D, Loquet A, Lange A, Reif B. Cryogenic solid state NMR studies of fibrils of the Alzheimer's disease amyloid-β peptide: perspectives for DNP. J Biomol NMR. 2013;56:359–63.

Lu M, Sarkar S, Wang M, Kraus J, Fritz M, Quinn CM, et al. 19F magic angle spinning NMR spectroscopy and density functional theory calculations of Fluorosubstituted Tryptophans: integrating experiment and theory for accurate determination of chemical shift tensors. J Phys Chem B. 2018;122:6148–55.

Mak-Jurkauskas ML, Bajaj VS, Hornstein MK, Belenky M, Griffin RG, Herzfeld J. Energy transformations early in the bacteriorhodopsin photocycle revealed by DNP-enhanced solid-state NMR. Proc Natl Acad Sci U S A. 2008;105:883–8.

Mariq M, Waugh J. NMR in rotating solids. J Chem Phys. 1979;70:3300–16.

McNally JM, Kreilick RW. Nuclear and electron spin relaxation in copper and nickel Tutton salts. J Phys Chem. 1981;86:421–8.

Munowitz M, Pines A. Multiple-quantum nuclear magnetic resonance spectroscopy. Science. 1986;1979(233):525–32.

Nadaud PS, Helmus JJ, Höfer N, Jaroniec CP. Long-range structural restraints in spin-labeled proteins probed by solid-state nuclear magnetic resonance spectroscopy. J Am Chem Soc. 2007;129:7502–3.

Ni QZ, Markhasin E, Can TV, Corzilius B, Tan KO, Barnes AB, et al. Peptide and protein dynamics and low-temperature/DNP magic angle spinning NMR. J Phys Chem B. 2017;acs.jpcb.7b02066:4997–5006. https://doi.org/10.1021/acs.jpcb.7b02066

Perez-Conesa S, Keeler EG, Zhang D, Delemotte L, McDermott AE. Informing NMR experiments with molecular dynamics simulations to characterize the dominant activated state of the KcsA ion channel. J Chem Phys. 2021;154:165102.

Polshakov VI, Birdsall B, Feeney J. Characterization of rates of ring-flipping in trimethoprim in its ternary complexes with *Lactobacillus casei* dihydrofolate reductase and coenzyme. Biochemistry. 1999;38:15962–9. https://doi.org/10.1021/bi9915263

Potapov A, Yau WM, Ghirlando R, Thurber KR, Tycko R. Successive stages of amyloid-β self-assembly characterized by solid-state nuclear magnetic resonance with dynamic nuclear polarization. J Am Chem Soc. 2015;137:8294–307.

Ringe D, Petsko GA. The 'glass transition' in protein dynamics: what it is, why it occurs, and how to exploit it. Biophys Chem. 2003;105:667–80.

Robustelli P, Stafford KA, Palmer AG. Interpreting protein structural dynamics from NMR chemical shifts. J Am Chem Soc. 2012;134:6365–74.

Rogawski R, McDermott AE. New NMR tools for protein structure and function: spin tags for dynamic nuclear polarization solid state NMR. Arch Biochem Biophys. 2017;628:102–13.

Rogawski R, Sergeyev IV, Zhang Y, Tran TH, Li Y, Tong L, et al. NMR signal quenching from bound biradical affinity reagents in DNP samples. J Phys Chem B. 2017;121:10770–81.

Sakellariou D, Brown SP, Lesage A, Hediger S, Bardet M, Meriles CA, et al. High-resolution NMR correlation spectra of disordered solids. J Am Chem Soc. 2003;125:4376–80.

Saliba EP, Sesti EL, Scott FJ, Albert BJ, Choi EJ, Alaniva N, et al. Electron decoupling with dynamic nuclear polarization in rotating solids. J Am Chem Soc. 2017;139:6310–3.

Sergeyev IV, Itin B, Rogawski R, Day LA, McDermott AE. Efficient assignment and NMR analysis of an intact virus using sequential side-chain correlations and DNP sensitization. Proc Natl Acad Sci U S A. 2017;114:5171–6.

Sergeyev IV, Quinn CM, Struppe J, Gronenborn AM, Polenova T. Competing transfer pathways in direct and indirect dynamic nuclear polarization magic anglespinning nuclear magnetic resonance experiments on HIV-1 capsid assemblies: implications for sensitivity and resolution. Magn Reson. 2021;2:239–49.

Sharpe S, Kessler N, Anglister JA, Yau WM, Tycko R. Solid-state NMR yields structural constraints on the V3 loop from HIV-1 Gp120 bound to the 447-52D antibody Fv fragment. J Am Chem Soc. 2004;126:4979–90.

Shikhov I, Arns CH. Temperature-dependent oxygen effect on NMR D-T2 relaxation-diffusion correlation of n-alkanes. Appl Magn Reson. 2016;47:1391–408.

Siegel JS, Anet FAL. Dichlorofluoromethane-d: a versatile solvent for VT-NMR experiments. J Org Chem. 1988;53:2629–30.

Siemer AB, Huang K-Y, McDermott AE. Protein linewidth and solvent dynamics in frozen solution NMR. PLoS One. 2012;7:e47242.

Smith AN, Long JR. Dynamic nuclear polarization as an enabling technology for solid state nuclear magnetic resonance spectroscopy. Anal Chem. 2015;88:122–32.

Su Y, Hong M. Conformational disorder of membrane peptides investigated from solid-state NMR line widths and line shapes. J Phys Chem B. 2011;115:10758–67.

Tran NT, Mentink-Vigier F, Long JR. Dynamic nuclear polarization of biomembrane assemblies. Biomolecules. 2020;10:1–22.

Tycko R. NMR at low and ultralow temperatures. Acc Chem Res. 2013;46:1923–32.

Wenk P, Kaushik M, Richter D, Vogel M, Suess B, Corzilius B. Dynamic nuclear polarization of nucleic acid with endogenously bound manganese. J Biomol NMR. 2015;63:97–109.

Yi X. Solid-state NMR Lineshape broadening at cryogenic temperatures. Columbia University; 2023.

How to cite this article: Sergeyev IV, Fritzsching K, Rogawski R, McDermott A. Resolution in cryogenic solid state NMR: Challenges and solutions. Protein Science. 2024; 33(7):e4803. https://doi.org/10.1002/pro.4803